Comparison between the interannual variability of snow parameters derived from SSM/I and the Ob river discharge

Manuela Grippa, Nelly Mognard, Thuy Le Toan

Comparison between the interannual variability of snow parameters derived from SSM/I and the Ob river discharge

M. Grippa [a,*], N. Mognard [b], T. Le Toan [a]

[a] *Centre d'Etudes Spatiales de la BIOsphère, 18 Av. E. Belin, 31401 Toulouse, France*
[b] *Laboratoire d'Etudes en G' eophysique et Oc' eanographie Spatiales, Toulouse, France*

This paper analyses the relationship between the interannual variations of snow depth and snowmelt date and river discharge measurements in the Ob river basin. The snow parameters are derived from passive microwave remote sensing measurements by SSM/I during the time period 1989–2001. We find a significant correlation between the snowmelt date and the runoff in May (correlation coefficient $R=-0.92$) and between the winter snow depth and the runoff in June ($R=0.61$) measured at the Ob estuary. These results validate the methods used to derive the interannual variability of the snow parameters, particularly the snow depth. In such vast and remote regions, this is fundamental for monitoring and predicting snow related flood events. Furthermore, the results obtained can be very useful to improve the description of the snow-runoff relationship in global hydrological models.

Keywords: Remote sensing; Snow depth; Snowmelt; Runoff; Microwave radiometry

1. Introduction

The Arctic river discharge is extremely important for the freshwater budget of the Arctic Ocean: its variability affects the salinity and the sea ice formation and it may have drastic effects on the thermohaline circulation (Aagaard & Carmack, 1989). Large-scale changes in freshwater flux to the Arctic Ocean have potentially important implications for ocean circulation and climate. Peterson et al. (2002) reported an increase of 7% in the average annual discharge of fresh water from the six largest Eurasian rivers to the Arctic Ocean between 1936 and 1999. This increase was correlated with changes in both the North Atlantic Oscillation and global mean surface air temperature.

One of the major factors that influences the river discharge at northern latitudes is the winter snow mass storage and its subsequent melt (Cao et al., 2002; Rango, 1997). Snow cover extent has been globally monitored using the series from NOAA/AVHRR since the early 1970s. Recent studies related the variability of the snow extent and the river runoff. Yang et al. (2003) showed a clear correspondence between the river stream flow and the seasonal snow cover extent changes from AVHRR. Warmer air temperatures in May have been related to the increase in snowmelt runoff for the Lena River and to the associated extremely high flood events (Yang et al., 2002). Yang et al. (2002) also investigated the dependence of the spring/summer runoff on the winter snow cover thickness: only a weak correlation ($R=0.14-0.27$ over the study period 1935–1999) has been found between winter precipitation, used as an indicator of the snowpack thickness, and the spring/summer season stream flow.

Even if these studies improved our knowledge of the spring discharge in Arctic regions, further work is needed to better understand the influence of the snowpack on river runoff. Moreover, the analysis of one of the major characteristics of the winter snowpack, the snow water equivalent or snow depth, over the river basin, is still

* Corresponding author.
E-mail address: manuela.grippa@cesbio.cnes.fr (M. Grippa).

missing. A better knowledge of the snow-runoff relationships is particularly important to improve global hydrological models that need validation regarding the simulation of this process (see, for example, Bowling et al., 2003). Also there is a growing need for monitoring the phenomena involved in snow-runoff processes, especially to predict high floods events that have a large impact on the socio-economy of the regions concerned. Since in remote regions, such as Siberia, in-situ measurements are becoming less and less available (given the high costs required to maintain them), remote sensing techniques provide a cost-effective means of observation.

Passive microwave measurements contain information on both snow extent and snow depth, independently of solar illumination and cloud cover (Ulaby et al., 1981). Several algorithms have been developed in the past to derive the snowpack characteristics from satellite passive microwave data at a global scale (Chang et al., 1987, 1976; Foster et al., 1997; Grippa et al., 2004; Kelly & Chang, 2003; Mognard & Josberger, 2002). Grippa et al. (2004) showed that the climatological characteristic features of snow depth fields in Northern Eurasia could be estimated only if a dynamic algorithm that takes into account the spatio-temporal variability of the snow grain size was implemented. However, for most areas, particularly in Northern Eurasia, the performance of the above methods in estimating the interannual variability of the snow parameters has not been evaluated, due to the scarcity of ground truth to compare with.

In this paper, we assess the interannual variability of the satellite-derived snow parameters using the monthly runoff measurements at the Ob river estuary as a proxy for the lack of in situ measurements. We analyse the relationship between the Ob river runoff and snow estimates derived from passive microwave remote sensing data over the 13-year period from 1989 to 2001. The work is thus driven by two main objectives:

(1) validate the interannual variations of the satellite-derived snow parameters (snowmelt date and snow depth) by comparison with runoff measurements;
(2) increase our understanding of the runoff dependence on the snowpack characteristics and on the snowmelt timings.

2. Study area and data sets

The Ob basin (Fig. 1) has the largest watershed of all Arctic rivers (2 975 106 km^2) and is the third largest contributor of fresh water to the Arctic Ocean with a mean annual flow of 402 km^3/year. A large part of the watershed is located within the Western Siberian plain: the absence of relief significantly affects the hydrographic network which presents a sharp asymmetry, with two-thirds of the watershed area (67% of the total area) located on the left-bank. An area of inner discharge (not providing inflow to the Ob River system) covers 15% of the watershed area (in white, between Irtysh and Novosibirsk, in Fig. 1). The Ob basin in the West Siberian plain is characterised by large flooded areas frequently described as the biggest world swamp. The region is abundant with lakes (over 450,000), mainly small lakes with surface area less than 1 km 2 and depths of 2–5 m. Given its large size (latitudes from 52°N to 68°N and longitudes from 61° to 94°), the basin includes different vegetation zones: the steppe in the south, taiga (mainly composed of secondary aspen/birch forests) in the central region and tundra in the northern areas.

The latitudinal extent of the Ob watershed results in the gradual snow melting from south to north during spring and in a smooth temporal variation of the discharge during the flooding period. The Ob discharge starts increasing in April, when the flood wave begins to break the ice cover, and reaches maximal values in May–June. During this time, large areas of the Ob basin are flooded. The discharge then gradually decreases until July–August, and in September–October, the flow is near base-level. About 75–80% of the annual flow is observed during the open water period before ice covers the river until the next spring (Kouraev et al., 2004).

Novosibirsk is the only reservoir on the Ob river: it is used for seasonal regulation with a volume that does not exceed 4.4 km^3 and does not affect the runoff variations measured at the estuary. The other reservoirs, located in the Irtysh basin, have an impact on the winter values of the runoff but their effect is negligible in spring when the discharge increases considerably due to snowmelt.

The melting of permafrost might influence the discharge of rivers flowing in northern Siberia such as the Yenisei and the Lena. This is not the case for the Ob river, since permafrost (discontinuous) affects only a small area in the north of the basin and the major contribution to the total discharge comes from more southern areas (Yang et al., 2002).

2.1. Data sets

2.1.1. SSM/I

The passive microwave radiances used to derive the snow parameters were measured by the Special Sensor Microwave/Imager (SSM/I), on board the Defence Meteorological Satellite Program satellite series since July 1987, DMSP F-8, F-11 and F-13 platforms. SSM/I is a multi-spectral radiometer with horizontally and vertically polarized channels at 19.35, 37 and 85.5 GHz and a vertically polarized channel at 22.235 GHz. This study employs the spectral gradient, which is the difference between the horizontally polarized 19 GHz and 37 GHz brightness temperatures. The radiometer sensitivity or noise equivalent temperature differential is of 0.41 K in the 19 GHz and of 0.37 K in the 37 GHz horizontally polarised channels. The

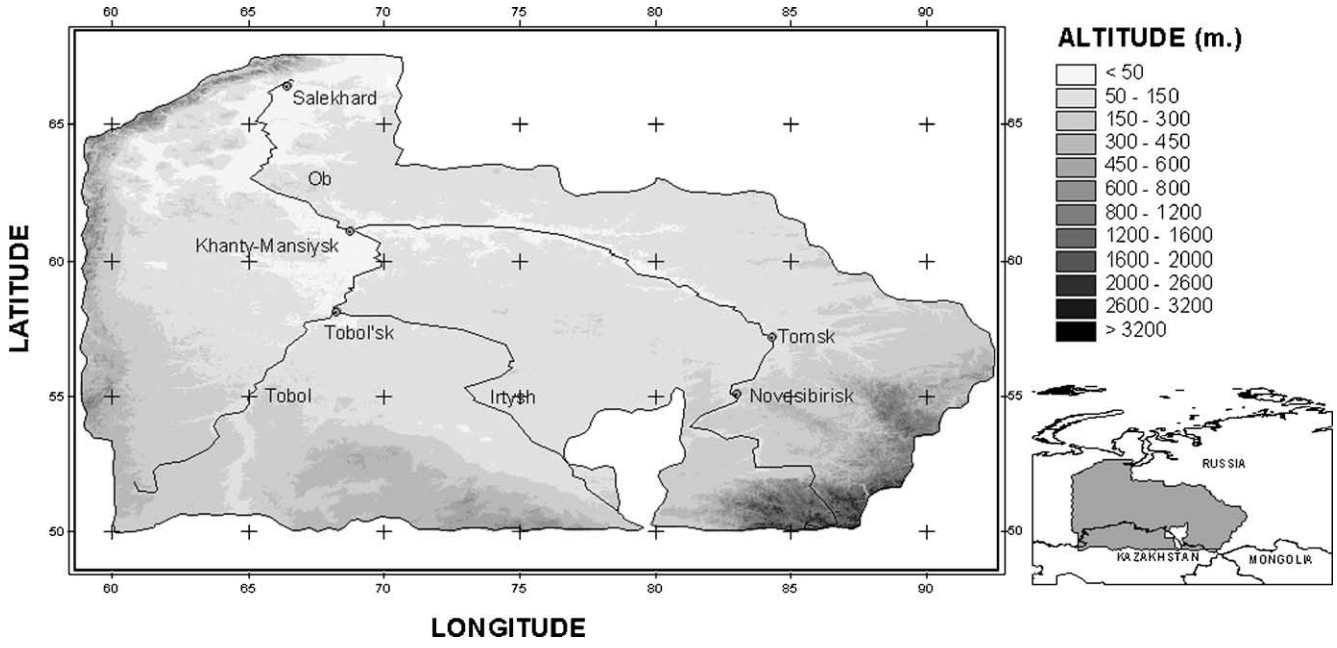

Fig. 1. Ob river basin.

National Snow and Ice Data Center (NSIDC) provided the SSM/I data mapped to the Equal Area SSM/I Earth Grid, with a 25 km^2 resolution. To minimise the spatial gaps resulting from the swath width, the daily data were averaged over pentads (5-day averages).

2.1.2. Ancillary data for the snow depth algorithm

The snow depth algorithm requires information on the surface and the ground temperatures. To obtain this information, we used the National Center for Environmental Prediction (NCEP) global air temperature reanalysis (Kalnay et al., 1996) and climatological ground permafrost temperature data from the International Institute for Applied System Analysis (Stolbovoi & McCallum, 2002). Both data sets were mapped to the same EASE-Grid projection used for the SSM/I measurements.

2.1.3. Ob river discharge measurements

The river discharge measured at the estuary is representative of the net precipitation (precipitation minus evaporation) over the river basin drainage area. The discharge measurements at the Salekhard station (located in the Ob

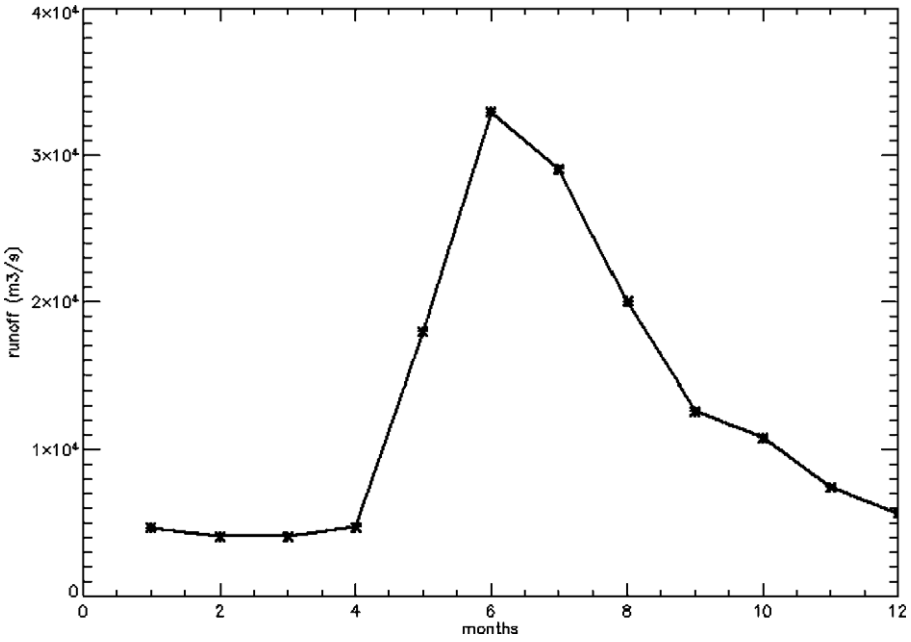

Fig. 2. Mean monthly runoff recorded at the Salekhard station (average values over 1989–2001).

estuary at the entrance to the Ob bay and the Kara sea) are part of the Roshydromet network. The stage height readings to the nearest centimeter were made daily, and cross-channel measurements of discharge for rating curve calibrations were made 25 to 30 times per year. With these frequent calibrations, estimates of daily discharge from the rating curves are accurate to ±5%. The mean monthly discharge values were obtained from R-ArcticNet web site [R-ArcticNet, 2003]. Fig. 2 shows the mean monthly runoff (average over 1989–2001) recorded at the Salekhard station: the seasonal runoff curve is in agreement with the general discharge behavior discussed at the beginning of Section 2.

2.1.4. Precipitation

The CPC Merged Analysis of Precipitation (CMAP) from the Climate Prediction Center is a monthly analysis of global precipitation on a $2.5 \times 2.5°$ latitude/longitude grid. The CMAP data set merges satellite and rain gauge data from a number of satellite sources (infrared and microwave) and rain gauge sources. The data set also uses precipitation from Numerical Weather Prediction models primarily to fill in gaps at high latitudes. Details on the component data sets as well as the method used to merge these data are provided by Xie and Arkin (1997).

3. Derivation of snow parameters from SSM/I measurements

The methods used to derive the parameters employed in this study are briefly described in the following subsections.

3.1. Timing of snow melt

The SSM/I 19 and 37 GHz horizontally polarized channels are used to detect the presence of snow on the ground. The 37 GHz radiance is scattered by the snow grains and the brightness temperature decreases as the snow depth increases, while the 19 GHz horizontally polarized channel is sensitive to the effects of ground temperature and atmospheric perturbations (such as atmospheric water vapour and clouds). When snow is absent, the 19 and 37 GHz channels measure similar brightness temperatures: the mean value of the spectral gradient over summer, when snow is absent, is of 3 K. The timing of snowmelt is therefore calculated as the date at which the spectral gradient is less then 3 K for at least 3 consecutive pentads.

3.2. Snow depth

A new dynamic algorithm has been developed to estimate snow depth for the Northern Great Plains of the USA (Josberger & Mognard, 2002; Mognard & Josberger, 2002) and has been recently adapted to the Siberian region (Grippa et al., 2004). The algorithm, based on the spectral gradient, takes into account the dependence of the microwave scattering on the snow grain size by considering the snow metamorphosis induced by the thermal gradient in the snowpack. For air temperatures well below freezing, temperature gradient metamorphism greatly accelerates the snow grain growth due to an upward transport of water vapour driven by the associated relative humidity gradient through the snowpack which rapidly forms large snow grains, commonly referred to as depth hoar (Sturm & Benson, 1997).

Snow depth, SD, at a given time t is calculated as (Josberger & Mognard, 2002):

$$\mathrm{SD}(t) = \alpha \frac{T_{\mathrm{ground}} - T_{\mathrm{air}}}{\mathrm{dSG}/\mathrm{d}t} \tag{1}$$

where T_{ground} and T_{air} are the temperatures below and above the snowpack, α is a constant and SG is the spectral gradient. In Josberger and Mognard (2002), the coefficient α was determined using an extensive network of in-situ snow depth measurements that is not available for Siberia. Here, we chose the value of α (equal to 3.5 for the whole study period) that allowed a good match with the climatological monthly data from the United States Air Force/Environmental Technical Applications Center (USAF/ETAC) in January (Grippa et al., 2004). The derivative of SG is calculated using a differential $\Delta\mathrm{SG}/\Delta t$. For each pentad, the time interval Δt is computed as the difference between the time t for the pentad considered and the time t_0 for the beginning pentad at the start of the snow season (Mognard & Josberger, 2002).

Eq. (1) can only be applied when the spectral gradient varies with time, corresponding to periods when the grain size and/or snow depth is rapidly varying. Grain size metamorphosis happens early in winter when thin snowpacks combined with cold air temperatures generate rapid crystal growth. To extend the snow depth computations past this time, we change to a linear static algorithm tuned to match the last snow depth estimate from each pixel (further details can be found in Grippa et al., 2004). The climatology (multi-year average over a long period) of the snow depth derived using this new method compared well with the USAF/ETAC snow depth climatology. Improved snow depth estimates were derived in comparison to those obtained by using a classical static algorithm (Chang et al., 1987) that does not consider spatio-temporal variation in the snowpack.

Validation is still needed to interpret the interannual variability estimated by the satellite passive microwave measurements. Since the SSM/I resolution is 25 km^2, the satellite-derived estimates can be only compared with in-situ data if a dense network of in-situ measurements is available. Chang et al. (2005) performed a statistical analysis to show that one in-situ measurement in a 100 by 100 km region provides a comparison with an uncertainty of 20 cm (for a range of snow depth values between 1.5 cm and 45.4 cm). Due to the sparse network

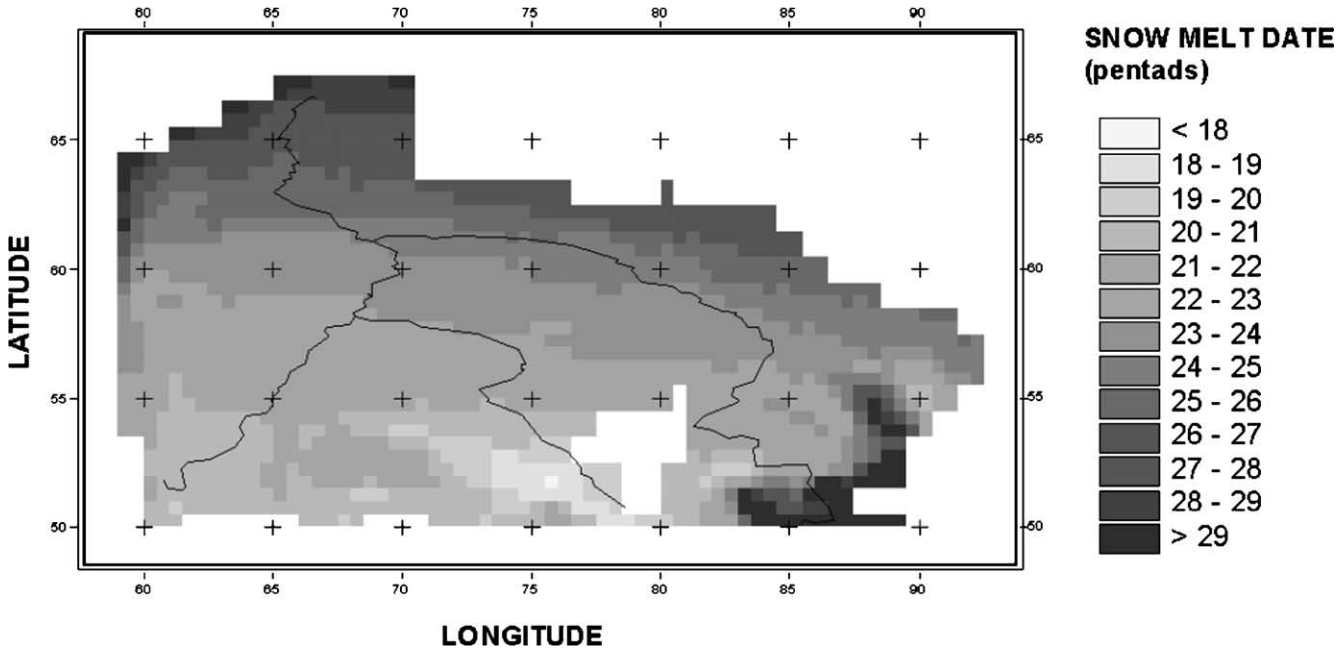

Fig. 3. Snowmelt date (pentad): average values over the study period 1989–2001.

of in-situ measurements in our study area, the alternative adopted in this paper is to use the river runoff at the estuary as a proxy for comparison with the interannual variations of the snowpack parameters.

4. Results and analysis

The snow parameters derived from SSM/I are shown in Figs. 3 and 4. The values reported are mean values over the study period 1989–2001. Fig. 3 shows the average snowmelt dates: in general, snow melts first in the south at the beginning of April (pentad 20) and finally in the north at the end of May (Fig. 3). Fig. 4 shows the winter snow depth: February is chosen as representative for the winter snow depth (similar results to those presented in this paper have been obtained by using the snow depth values derived for the month of March). Snow depth varies between 20 and 70 cm with a minimum in the southwest and maxima in the northeast and in the north-west of the region under study. There is no evident correlation between the dates of snowmelt and the snow depth values: a thicker snowpack

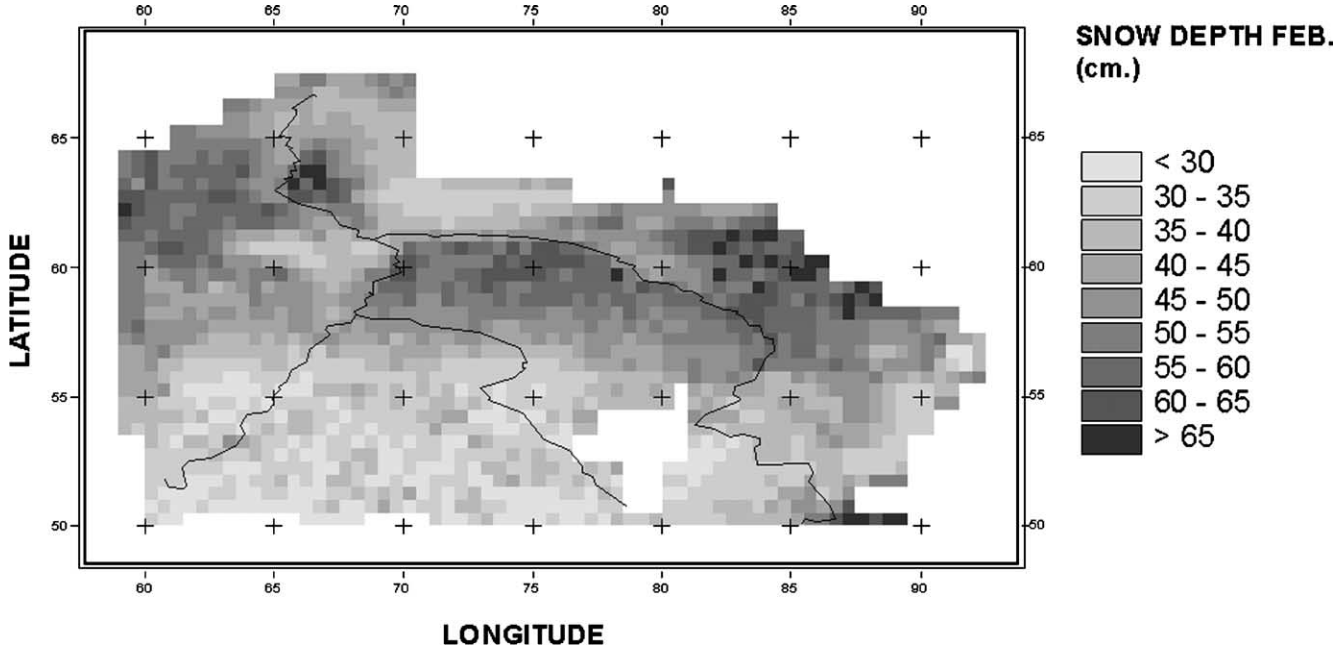

Fig. 4. Winter snow depth (February): average values over the study period 1989–2001.

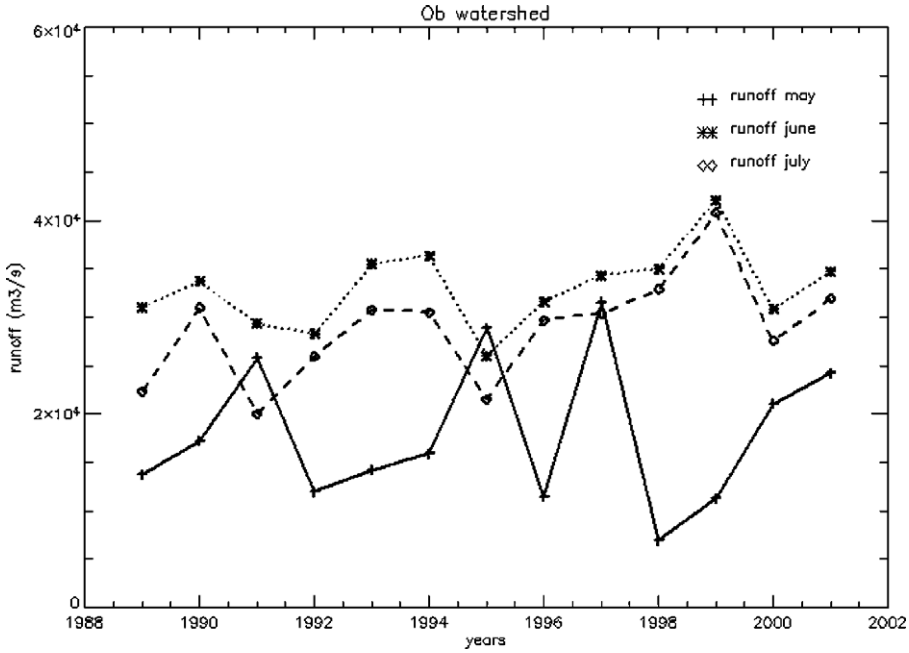

Fig. 5. Interannual variations of monthly runoff between May and July. Average values for the entire Ob river basin.

should increase the duration of the melting process, delaying the timing of the snow disappearance. In fact, snowmelt is mostly driven by the air temperature pattern that masks the influence of the snowpack thickness.

4.1. Interannual variability

Fig. 5 shows the temporal evolution between 1989 and 2001 of the monthly runoff at Salekhard for the months between May and July. The runoff reaches the highest values in June (as also shown in Fig. 2) and presents the largest interannual variations in May, the month most affected by snowmelt.

Figs. 6 and 7 show the temporal evolution of the snow estimates (snowmelt timing and snow depth) and of precipitation (monthly values between April and July). For each year, the values reported are spatially averaged over the entire Ob river basin. The average date of snowmelt shows

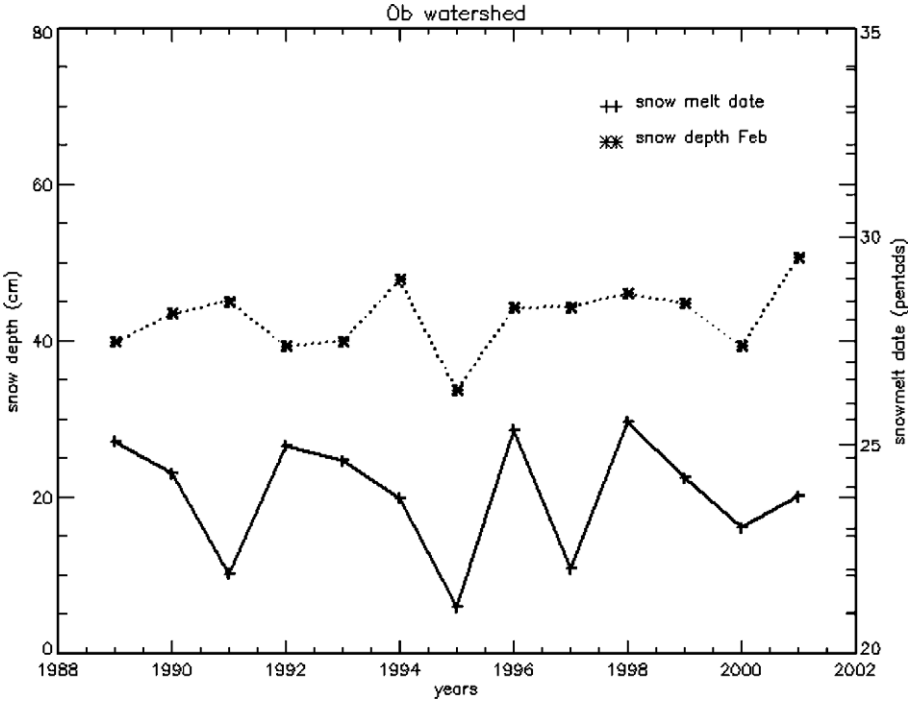

Fig. 6. Interannual variations of the snow parameters (snow melt date and winter snow depth). Average values for the entire Ob river basin.

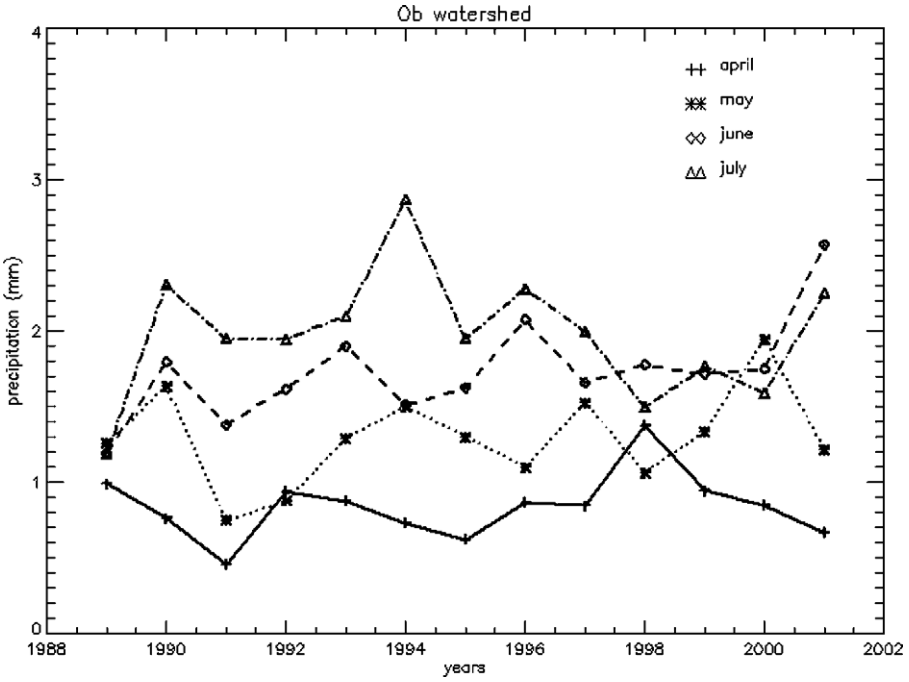

Fig. 7. Interannual variations of monthly precipitation between April and July. Average values for the entire Ob river basin.

interannual variations of about 15 days (between pentad 27 and 30, corresponding to mid and end of May) that are mostly dependent on air temperature variations. We found a significant correlation ($R=-0.91$) between the interannual variations of snowmelt dates and the interannual variations of mean temperatures in April (calculated from the NCEP global air temperature reanalysis (Kalnay et al., 1996)).

Monthly precipitation presents a large interannual variability but the general trend is an increase in precipitation from April to July.

4.2. Correlation between runoff, snow and precipitation

Table 1 shows the correlation coefficients (calculated by linear regression) between the runoff and the snow and precipitation variability for the period 1989–2001. Coefficients with absolute values higher than 0.55 are statistically significant at 95% confidence level (the level of significance for two-tailed test is $P \leq 0.05$).

The spring runoff in May (Fig. 5) is extremely correlated to the snowmelt date (Fig. 6) and to a lesser extent to precipitation in the previous month (Fig. 7). In fact, the water released by the snowpack after melting produces a sharp increase in the runoff values (see Fig. 2). Since snowmelt happens on average in May, this is reflected onto the May runoff values: the earliest the snowmelt, the earliest the sharp increase in the water discharge, the highest the mean values of runoff in May. The runoff in June (Fig. 5) is significantly correlated to the winter snow depth (Fig. 6): a deeper snowpack produces a larger amount of water redirected towards the rivers. The regression results for the runoff in May and June and respectively snowmelt date and snow depth are shown in Fig. 8. We also performed a multicorrelation analysis to investigate the runoff dependence on both snowmelt and snow depth. The multicorrelation coefficients obtained ($R=-0.92$ for the runoff in May and $R=0.62$ for the runoff in June) were very similar to those obtained by correlating separately the runoff in May to snowmelt and the runoff in June to snow depth (see Table 1). This confirms that the effects of snowmelt and snow depth on the monthly runoff are independent.

Table 1
Summary of the correlations (R-values) between the monthly runoff and the SSM/I derived parameters (calculated by a linear regression as shown Fig. 8 for the May runoff vs. the snowmelt date and the June runoff vs. the February snow depth)

Runoff	Precipitation (Previous month)	Snowmelt date	Snow depth (Feb) New formulation	Snow depth (Feb) Classical formulation
May	0.71	−0.92	0.12	0.09
June	0.25	−0.33	0.61	0.16
July	0.50	−0.39	0.50	0.23

The influence of the snowpack on the runoff becomes less evident in July when the increase in precipitation during June also plays a role (see Table 1 and Figs 5–7). The values of the correlation between the monthly runoff and precipitation during the same month were lower than those between the monthly runoff and precipitation during the previous month and therefore were not reported.

Figs. 9 and 10 show the runoff anomalies (calculated as the difference between the yearly runoff values and the multi-year average) respectively in May and June along with the anomalies in snowmelt date and snow depth. The

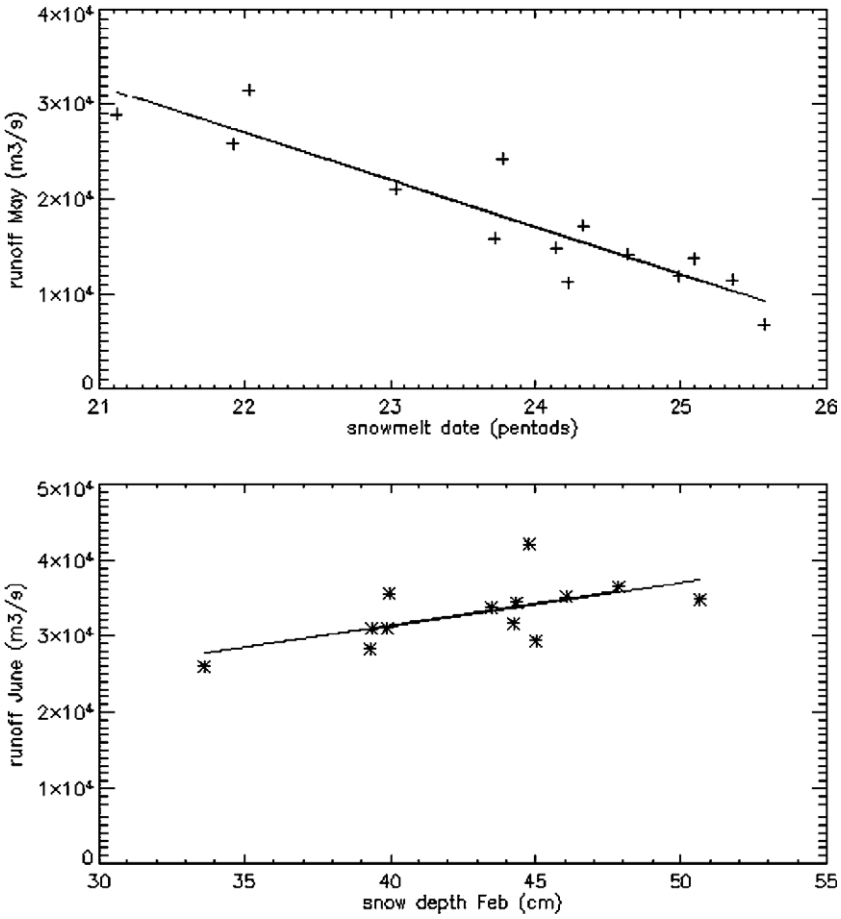

Fig. 8. Linear regression results. Top: May runoff vs. snowmelt date; bottom: June runoff vs. February snow depth.

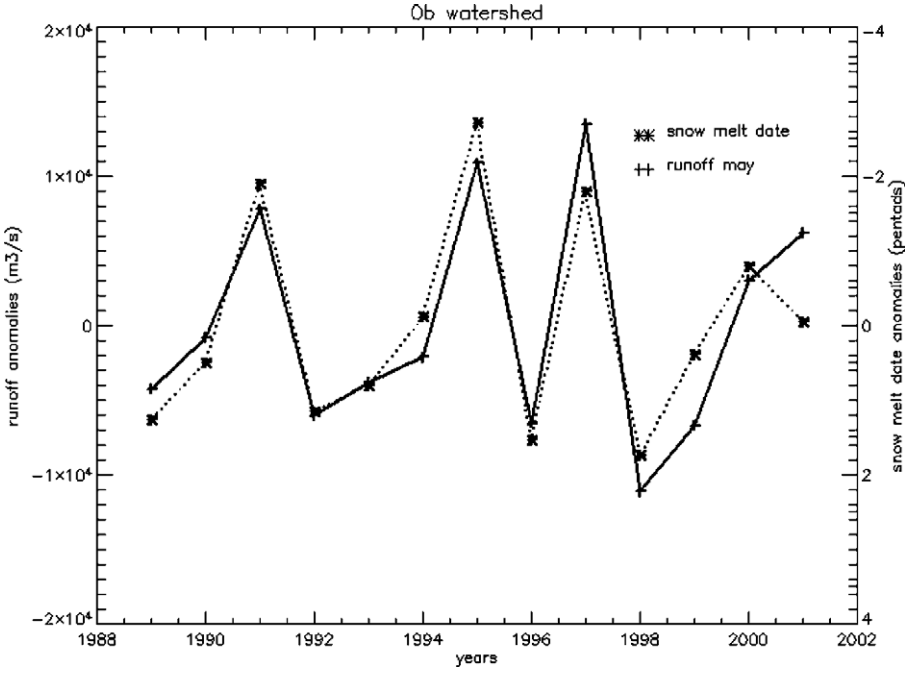

Fig. 9. Anomalies of May runoff and snowmelt date.

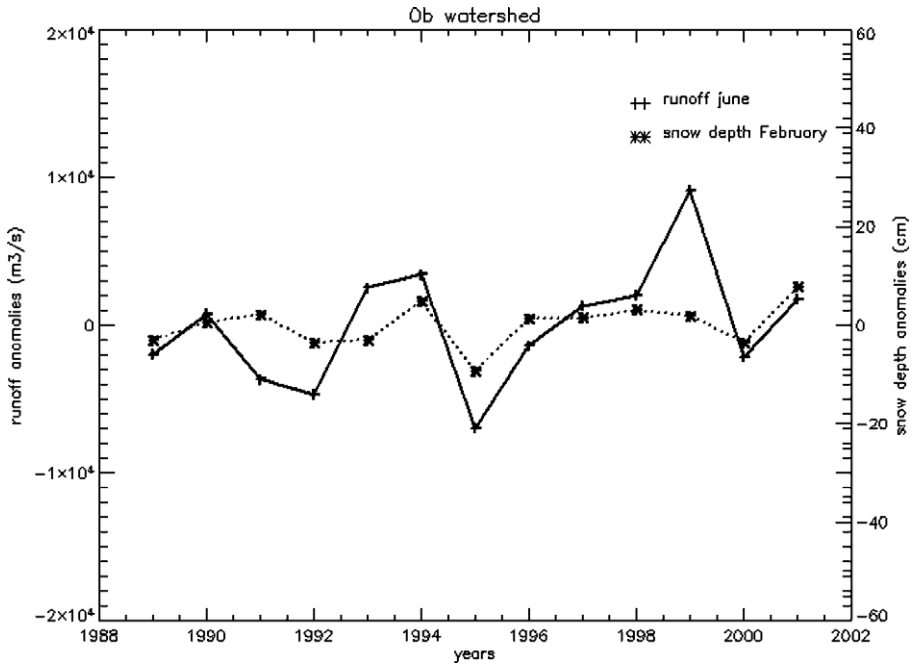

Fig. 10. Anomalies of June runoff and winter snow depth.

relation between snowmelt date and May runoff anomalies (Fig. 9) is striking and it does not depend on the amount of water available in the snowpack: this means than even in years of low snow fall, when snowmelt starts, there is always enough water to provide a significant increase in runoff. The amount of water available in the snowpack becomes important later (in June): the years with less snowfall are characterised by negative anomalies of the June runoff (Fig. 10). For example, in 1995, snowmelt is early giving rise to a runoff peak in May, but snow depth is low resulting in a sharp decrease in the June runoff. The maximum value of the June runoff, reached in 1999, does not seem to be explained either by a significantly positive anomaly in the snow depth or by a significantly high value of precipitation. We also calculated the runoff sum for May and June which does not correlate better with the snow depth, the mean runoff in May being almost exclusively influenced by the timing of the snowmelt.

The results obtained provide validation of the methods used to derive the snow estimates, particularly snow depth. The last column in Table 1 reports the correlation coefficients between the runoff and the snow depth calculated using a classical static algorithm (Chang et al., 1987) that does not take into account the snow metamorphosis due to temperature: no significant correlation is found in this case and the *R*-values are always lower than those obtained when applying the dynamic algorithm described in Section 3.2.

5. Conclusions and perspectives

The interannual variations of monthly runoff at the Ob estuary have been compared to the variations of snow parameters derived from remote sensing passive microwave measurements over the Ob basin. A significant correlation has been found between the runoff in May and the snowmelt timing and the runoff in June and the winter snow depth. These results allow a cross-validation of the SSM/I derived snow parameters, snow melt timing and snow depth, and strongly encourage the use of passive microwave remote sensing to monitor snow in boreal regions. This has implications in the context of global change. Monitoring the snowpack variability in the Northern river basins is fundamental to estimate the variability of freshwater flux to the Arctic Ocean. Moreover, changes in snow depth and snowmelt timings affect the surface albedo with feedback on the climate at regional and global scale and they also have an impact on the vegetation development and the related carbon cycle.

The snow depth retrieval method can be generalised to analyse other large river basins in the Arctic if global data on the ground temperatures are available (the IIASA data employed for this study are only provided for the former Soviet Union).

The analysis reported in this paper may be very useful to improve the description of the snow-runoff relations in hydrological models. Further work has to be done to investigate the relationships found in this study on a shorter time scale (for example, on a daily base).

Acknowledgements

This work has been supported by the Siberia-II project in the framework of the 5th EU research network. The authors wish to acknowledge Alexei V. Kouraev (LEGOS, Toulouse, France) and Aaron Boone (Meteo France, Toulouse, France) for the interesting and helpful discussions on the subject.

References

Aagaard, K., & Carmack, E. C. (1989). The role of sea ice and other fresh water in the arctic circulation. *Journal of Geophysical Research*, *94*(C10), 14485–14498.

Bowling, L. C., Lettenmaier, D. P., Nijssen, B., Graham, L. P., Clark, D. B., & El Maayar, M., et al. (2003). Simulation of high-latitude hydrological processes in the TorneKalix basin: PILPS Phase 2(e): I. Experiment description and summary intercomparisons. *Global and Planetary Change*, *38*, 1–30.

Cao, Z., Wang, M., Proctor, B., Strong, G., Stewart, R., & Ritchie, H., et al. (2002). On the physical processes associated with the water budget and discharge over the Mackenzie basin during the 1994/95 water year. *Atmosphere-Ocean*, *40*(2), 125–143.

Chang, A. T. C., Foster, J. L., & Hall, D. K. (1987). Nimbus-7 SMMR derived global snow cover parameters. *Annals of Glaciology*, *9*, 39–44.

Chang, A. T. C., Gloersen, P., Schmugge, T., Wilheit, T., & Zwally, H. J. (1976). Microwave emission from snow and glacier ice. *Journal of Glaciology*, *16*(74), 23–39.

Chang, A. T. C., Kelly, R., Josberger, E. G., Armstrong, R. L., Foster, J. L., & Hall, D. K., et al. (2005). Analysis of ground-measured and passive microwave derived snow depth variations in mid-winter across the Northern Great Plains. *Journal of Hydrometeorology*, *6*, 20–33.

Foster, J. L., Chang, A. T. C., & Hall, D. K. (1997). Comparison of snow mass estimates from a prototype passive microwave snow algorithm, a revised algorithm and a snow depth climatology. *Remote Sensing of Environment*, *62*, 132–142.

Grippa, M., Mognard, N. M., Le Toan, T., & Josberger, E. G. (2004). Siberia snow depth climatology derived from SSM/I data using a combined dynamic and static algorithm. *Remote Sensing of Environment*, *93*, 30–41.

Josberger, E. G., & Mognard, N. M. (2002). A passive microwave snow depth algorithm with a proxy for snow metamorphism. *Hydrological Processes*, *16*(8), 1557–1568.

Kalnay, E., Kanamitsu, M., Kistelr, R., Collins, W., Deaven, D., & Gandin, L., et al. (1996). The NCEP/NCAR 40-year reanalysis project. *Bulletin of the American Meteorological Society*, *77*(3), 437–471.

Kelly, R. E. J., & Chang, A. T. C. (2003). Development of a passive microwave global snow depth retrieval algorithm for Special Sensor Microwave Imagery (SSM/I) and Advanced Microwave Scanning Radiometer-EOS (AMSR-E) data. *Radio Science*, *38*(4), 1–11.

Kouraev, A. V., Zakhararova, E. A., Samain, O., Mognard, N. M., & Cazenave, A. (2004). Ob river discharge from TOPEX/Poseidon satellite altimetry. *Remote Sensing of Environment*, *93*, 238–245.

Mognard, N. M., & Josberger, E. G. (2002). Northern Great Plains 1996/97 seasonal evolution of snowpack parameters from satellite passive microwave measurements. *Annals of Glaciology*, *34*, 15–23.

Peterson, B. J., Holmes, R. M., McClelland, J. W., Vorosmarty, C. J., Lammers, R. B., & Shiklomanov, A. I., et al. (2002). Increasing river discharge to the Arctic Ocean. *Science*, *298*, 2171–2173.

Rango, A. (1997). Response of aeral snow cover to climate change in a snowmelt-runoff model. *Annals of Glaciology*, *25*, 232–236.

R-ArcticNet v. 2.0 (2003). A Regional, Electronic, Hydrographic Data Network For the Arctic Region, http://www.r-arcticnet.sr.unh.edu/

Stolbovoi, V., & McCallum, I. (2002). CD-ROM land resources of Russia. International Institute for Applied System Analysis and the Russian Academy of Science, Laxenburg, Austria.

Sturm, M., & Benson, C. S. (1997). Vapor transport, grain growth and depth-hoar development in the subarctic snow. *Journal of Glaciology*, *43*(143), 42–59.

Ulaby, F. T., Moore, R. K., & Fung, A. (1981). *Microwave remote sensing*. Reading, Mass.: Addison-Wesley-Longman.

Xie, P., & Arkin, P. A. (1997). Global precipitation: A 17-Year monthly analysis based on gauge observations, satellite estimates, and numerical model outputs. *Bulletin of the American Meteorological Society*, *78*, 2539–2558.

Yang, D., Kane, D. L., Hinzman, L. D., Zhang, X., Zhang, T., & Ye, H. (2002). Siberian Lena river hydrologic regime and recent change. *Journal of Geophysical Research*, *107*(D23), 4694 doi: 10.1029/2002JD002542.

Yang, D., Robinson, D., Zhao, Y., Estilow, T., & Ye, B. (2003). Streamflow response to seasonal snow cover extent changes in large Siberian watersheds. *Journal of Geophysical Research*, *108*(D18), 4578 doi: 10.1029/2002JD003149.